SWEENEY CONVENTION CENTER / SANTA FE / NEW MEXICO
3 - 5 JUNE 1992

Rock Mechanics Proceedings of the 33rd U.S. Symposium

Edited by
J.R.TILLERSON & W.R.WAWERSIK
Sandia National Laboratories, Santa Fe

OFFPRINT

A.A.BALKEMA / ROTTERDAM / BROOKFIELD / 1992

Rock Mechanics, Tillerson & Wawersik (eds) © 1992 Balkema, Rotterdam. ISBN 90 5410 045 1

Immiscible fluid flow in a fracture

Laura J. Pyrak-Nolte, Dan Helgeson & Guy M. Haley
Department of Earth & Atmospheric Sciences, Purdue University, W. Lafayette, Ind., USA
James W. Morris
Department of Chemistry, Purdue University, West Lefayette, Ind., USA

ABSTRACT: A stratified continuum model is used to generate fracture void geometries to investigate the effect of trapping on immiscible flow through a fracture. For a wetting phase invading a fracture initially saturated with a non-wetting phase, trapping of the non-wetting phase occurs in local maxima that are surrounded by smaller apertures. Trapping of the non-wetting phase results in high residual saturation and low values of wetting phase relative permeability. An epoxy cast of a natural fracture was used to visually observe trapping in a fracture.

1 INTRODUCTION

Energy sources such as coalbed methane, geothermal springs, and oil fields often occur in fractured reservoirs and involve the flow of two phases in fractures. Multiphase flow through fractures is also a concern for contaminant transport and the isolation of radioactive waste. An underlying question of the movement of two fluids through a fracture is how the fracture geometry affects residual saturation and relative permeabilities. In reviewing the literature, few experimental measurements have been made of relative permeability in fractures (Barton, 1972; Merrill, 1975; Bawden & Rogiers, 1985). These experiments were performed on artificial fractures, or fractures represented by parallel glass plates. Several investigators have undertaken theoretical investigations of multiphase flow in fractures. Some models involve the use of capillary theory to study multiphase flow through fractures idealized as parallel plates (Evans, 1983; Evans & Huang, 1983; Rasmussen et al., 1985) or wedge-shaped fractures with continuously varying apertures [Rasmussen, 1987]. Pruess & Tsang (1990) numerically analyzed relative permeabilities of a rough-walled fracture for a lognormal aperture distribution and various spatial correlations. They found that relative permeabilities are sensitive to the nature and range of spatial correlation of the apertures. Pyrak-Nolte et al. (1990) examined unsaturated flow in single fractures for the case of a non-wetting phase invading a wetting phase fluid (such as mercury injected into a fracture saturated with air in rock).

Pruess & Tsang (1990) investigated numerically the effect of different aperture distributions on two-phase flow through a fracture using global accessibility. Accessibility determines which apertures will be occupied by which phase. For wetting-phase invasion, global accessibility allows all sites to be occupied even if they are not connected to the inlet. This paper will examine the effect of global accessibility compared with inlet accessibility with trapping for a wetting phase invading a fracture initially saturated with a non-wetting phase. Numerical and experimental results will be presented.

2 EXPERIMENT

A laboratory study was undertaken to observe trapping in natural fractures. To visually examine the distribution of each phase in the fracture, an epoxy cast of a natural fracture in granite was made. The natural fracture measured 52 mm in diameter. A mold of each fracture surface was made using Wood's metal, i.e., a Bismuth-based, low melting point metal. The molds of each surface were filled with epoxy and allowed to solidify. After the epoxy solidified, the mold with epoxy was placed in boiling water to remove the Wood's metal. The two casts of the fracture surfaces were placed together to form the fracture. The sides of the specimen were sealed except for two ports for the fluid inlet and outlet. These ports were approximately 3.18×10^{-3} m in diameter and were diametrically opposed. The fracture was first saturated with a non-wetting phase (a dye with a surface tension = 50.7 dynes/cm, and a viscosity = 1.57 cp) using an inlet pressure of 635 Pa. The wetting phase was a mineral oil (surface tension = 30.3 dynes/cm; viscosity = 28.05 cp). The oil was invaded into the dye-saturated fracture using an inlet pressure of 1044 Pa. The velocity of invasion of the oil was approximately 1.8×10^{-5} m/s and was kept at this rate to avoid viscous fingering (Wong, 1988). Once a connected path across the cast was formed and stabilized, the oil flowrate was measured at 5.0×10^{-9} m/s. The entire invasion of oil into a dye-saturated fracture was captured on video tape. Figure 1 is a drawing from a video image when the distribution of the wetting phase (oil) and the non-wetting phase (dye) reached steady-state. In the image, large regions of trapped dye (non-wetting phase) are observed and the oil (wetting phase) flow path is tortuous.

3 MODEL

In this analysis of the effect of trapping on two-phase flow, fracture void topologies are generated using a stratified continuum model. A continuum model is used because the distribution of void apertures is continuous and there is no underlying lattice structure. The simulated fracture void patterns are based on a fractal construction that produces spatially correlated aperture densities with an approximately log-normal size distribution.

Figure 1. Oil (wetting phase: black) invaded into a fracture saturated with dye (non-wetting phase: white) under capillary pressure effects.

Details of the model and construction of the pattern can be found elsewhere in the literature (Pyrak-Nolte et al., 1988; Nolte and Pyrak-Nolte, 1991). Figure 2 is a contour map of the aperture distribution from a fracture void pattern generated using the stratified continuum model. The pattern is based on a five-tier model (T = 5) with twelve points per tier (N=12) and a scale factor of B=2.37 between tiers. The white regions represent contact area and increasing shades of gray represent increasing aperture. The contour interval is 20 units of aperture. This pattern represents a fracture under low stress because there is very little contact area (~ 1%). The maximum aperture is 264 units. In this analysis, five different patterns were generated using the same values of T, N, and B.

4 FLUID ACCESSIBILITY

The relationship between capillary pressure and saturation of a fracture will affect how two phases are introduced into a fracture. We assume that the distribution of each phase in the fracture will depend only on capillary pressure effects and neglect the effects of buoyant and viscous forces. The configuration of the flow paths of the wetting and non-wetting phases are based on the local fracture geometry and are independent of global pressure gradients. We make the assumption that the area occupied by each phase is directly dependent on the capillary pressure. The capillary pressure is taken to be inversely proportional to the local aperture. When the non-wetting phase is in a small aperture, this corresponds to a high capillary pressure. The simulations begin with the fracture saturated with a non-wetting phase. Flow is assumed to occur left to right in simulations with zero-flow boundary conditions at the top and bottom of the patterns.

Global accessibility and inlet accessibility with trapping are used to introduce each

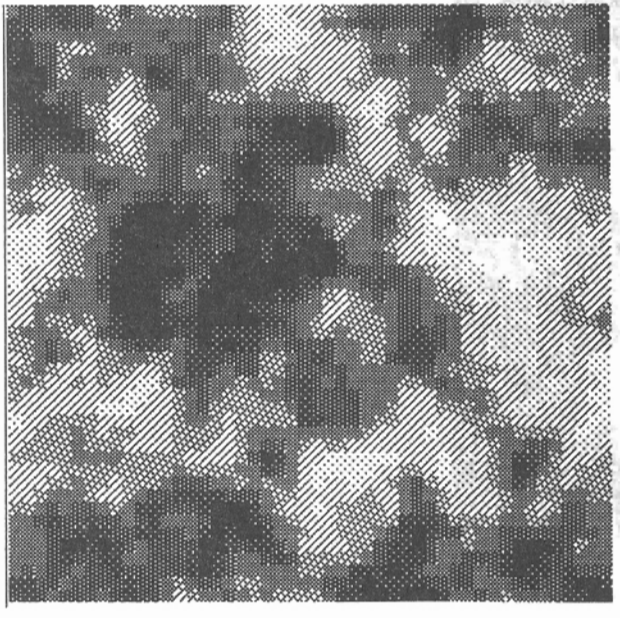

Figure 2. Aperture contour map of a simulated fracture void geometry using the stratified continuum model. White regions represent areas of contact. Increasing shades of gray represent increasing aperture. Contour interval: 20 units.

phase into the fracture. For wetting-phase invasion, global accessibility allows all sites of a given aperture or less to be occupied even if they are not connected to the inlet. Inlet accessibility with trapping refers to the approach where wetting phase is introduced from the inlet of the fracture simulation and occupies sites with wetting phase for all sites of aperture b or less connected to the invading front, unless the non-wetting phase occupying that site is surrounded by the wetting phase. If the non-wetting phase is surrounded by the wetting phase, the non-wetting phase is trapped and no longer participates in the flow and can never be occupied by the wetting phase.

Figure 3 shows the distribution of the wetting phase and non-wetting phase in a fracture using inlet accessibility with trapping at breakthrough (Figure 3 top) and at maximum possible saturation (Figure 3 bottom). Breakthrough occurs when the first connected path of wetting phase is formed that spans the fracture. Black in Figure 3 represents the invading wetting phase and white regions represent the non-wetting phase. Gray regions represent rock-to-rock contact. Trapping causes a high value of residual

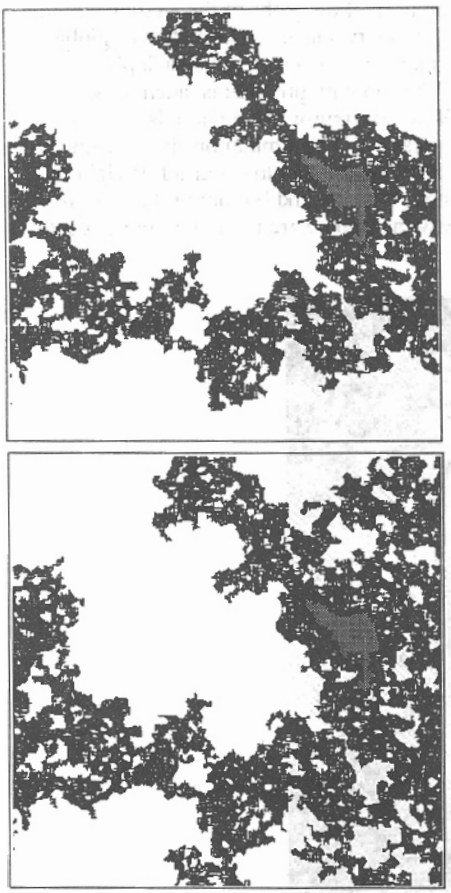

Figure 3. Invasion of wetting phase (black) into the fracture saturated with non-wetting phase at breakthrough (top) and for maximum saturation (bottom). The aperture distribution is shown in Figure 2. Contact area is represented by gray regions.

saturation of non-wetting phase in the fracture. If global accessibility were used, the entire pattern in Figure 3(bottom) would be black. Because of the correlated and continuous nature of the void geometry of the simulated fracture, the non-wetting phase becomes trapped in regions of local maxima. Regions of local maxima are surrounded by voids of smaller apertures through which the wetting phase preferentially flows. The amount of trapping in a fracture depends on the spatial correlations of the apertures in the fracture.

5 CAPILLARY PRESSURE -SATURATION RELATION

The capillary pressure-saturation is calculated by assuming that the capillary pressure is inversely proportional to the aperture of the fracture. Throughout the simulation the volume and area of the wetting phase were recorded as a function of invaded aperture size as the wetting phase was introduced into the fracture. The wetting phase saturation is calculated by dividing the volume of wetting phase in the simulated fracture by the total volume. Figure 4 shows the average for five fracture void simulations for both global accessibility and inlet accessibility with trapping. The capillary pressure curve for a log-normal aperture distribution in a fracture is similar to the customary j function for three-dimensional porous media (Pruess & Tsang, 1990). The important feature of Figure 4 is the difference between the results for inlet accessibility with trapping and global accessibility. Trapping of the non-wetting phase by the wetting phase has a dramatic effect on the capillary pressure curves for a single fracture. Because of trapping, lowering the capillary pressure will never result in complete wetting phase saturation. For the simulations, at the lowest capillary pressure, the maximum wetting phase saturation is roughly thirty-five percent.

6 FLOW & RELATIVE PERMEABILITY

To determine the relative permeability of each phase in the simulated fractures, relative flow of each phase through the fracture is evaluated. Relative fluid flow through the

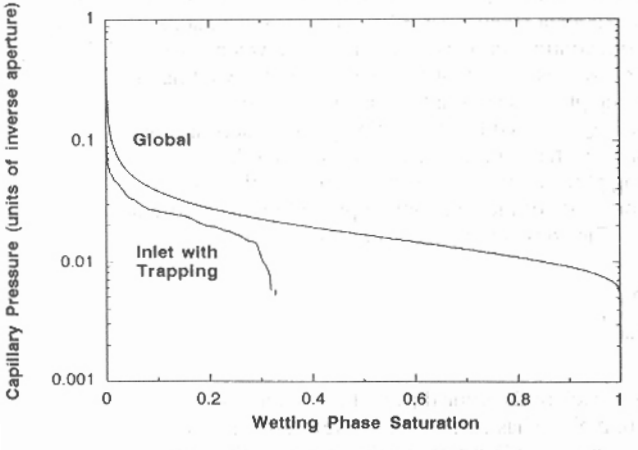

Figure 4. Capillary pressure as a function of wetting phase saturation for global accessibility and inlet accessibility with trapping.

fracture is calculated for each increment of capillary pressure (increment of aperture) assuming steady-state equilibrium conditions. In calculating fluid flow through the fracture, a zeroth order approach is taken that includes only the simplest dependences. For determining the wetting phase flow, Q_w, "cubic law" (Witherspoon et al., 1980) behavior is assumed to describe the local dependence of fluid flow on aperture. The two-dimensional critical behavior is included by a scaling law that describes changes in tortuosity.

$$Q_w = \frac{\Delta P}{\Delta L}\frac{W C}{\mu_w} b_{eff}^3 (a_w - a_{cw})^t \qquad (1)$$

where b_{eff} is the effective aperture of the wetting phase critical neck and is given by

$$b_{eff} = \frac{\text{Volume Invaded}}{\text{Area Invaded}} + (b_{cw} - \frac{\text{Critical Volume Invaded}}{\text{Critical Area Invaded}})$$

and the constant of proportionality, C, is given by

$$C = \frac{b_{crpatr}^3}{b_{eff100\%}^3 (a_{100\%} - a_{cw})}$$

where

Q - Flow	$\Delta P/\Delta L$ - Pressure Gradient
b - Aperture	a - Normalized Area
w - Wetting Phase	c - Critical neck of either w or nw
nw - Non-Wetting Phase	100% - 100% saturation
crpatr - Critical Neck of Pattern	μ - Viscosity
W - Fracture Width	t - critical exponent

The area, a_w, occupied by the wetting phase is normalized by the area of the entire simulated fracture. The critical area, a_{cw}, is the normalized area of the wetting phase at threshold, and t is a critical exponent taken to be t=1.9 for these simulations. The critical exponent for standard random continuum percolation ranges between $1.7 < t < 2.7$ (Halperin et al., 1985). Tortuosity is important for determining the wetting phase flow because the path of the wetting phase is constantly changing with changes in saturation. An effective critical aperture, b_{eff}, is used for the wetting phase to account for the parallel flow paths that are established as the wetting phase is allowed into larger apertures.

Because the non-wetting phase dominates the critical path of the pattern and only flows along this path, the tortuosity of the non-wetting phase flow path does not change with a change in saturation. The non-wetting phase flow is given by

$$Q_{nw} = \frac{\Delta P}{\Delta L}\frac{W}{\mu_{nw}} b_{cnw}^3 (1 - \frac{b_w}{b_{cnw}}) \qquad (2)$$

where b_{cnw} is the critical neck of the critical path of the fracture simulation, and b_w is the largest aperture the wetting phase has entered for a given capillary pressure. The quantity $\{1 - (b_w / b_{cnw})\}$ in equation (2) represents the change in the width of the non-wetting phase critical neck as the wetting phase is allowed into larger apertures. Equations (1) and (2) differ slightly from the equations put forth by Pyrak-Nolte et al.

(1990) to model the alternate process for the displacement of a wetting phase by a non-wetting phase.

Relative permeabilities of each phase in the fracture void simulations were determined from relative flow values:

$$\frac{k_w}{k_{tot}} \propto \frac{Q_w}{Q_{tot}} \qquad \text{and} \qquad \frac{k_{nw}}{k_{tot}} \propto \frac{Q_{nw}}{Q_{tot}}$$

where

$$Q_{tot} = \frac{\Delta P}{\Delta L} \frac{W}{\mu_w} b^3_{crpatr}$$

where k_w is the permeability of the wetting phase, and k_{tot} is the single phase permeability. Flow for each phase was normalized by the flow through the simulation for complete saturation by the wetting phase. The global pressure gradient was assumed equal for both phases. Viscosities are based on the values for methane (108.7 x 10-6 poise) and water (0.01 poise). In coal, methane is the wetting phase and water is the non-wetting phase because coal is hydrophobic (Fuerstenau et al., 1990).

Figure 5 shows the effect of trapping on the relative permeabilities of each phase. Trapping results in a maximum wetting phase permeability of six percent for a maximum wetting phase saturation of thirty-five percent. The high residual saturation is a direct result of the fracture topologies. Because of the correlated geometry of the simulated fracture, the non-wetting phase becomes trapped in regions of local maxima. Regions of local maxima are surrounded by voids of smaller apertures through which the wetting phase preferentially flows.

7 CONCLUSIONS

From the experiments, trapping of a non-wetting phase by a wetting phase is observed for a natural fracture. This phenomenon can be modeled based on fundamental physical

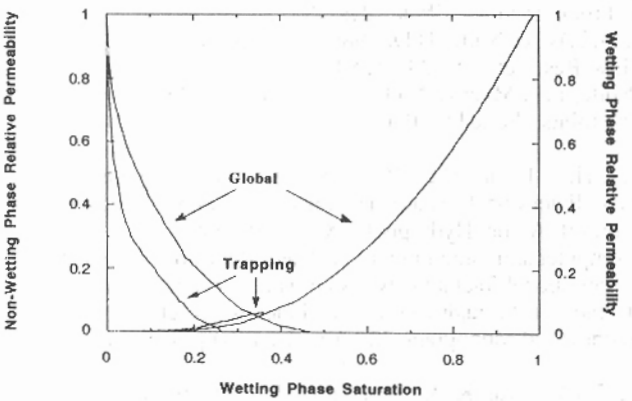

Figure 5. Relative permeabilities as a function of wetting phase saturation for global accessibility and inlet accessibility with trapping.

principles. The significant effect of trapping on the flow of two immiscible fluids in a fracture is directly related to the fracture void geometry. For the flow of a gas and water, such as in coalbed methane production, trapping of the water by methane will significantly reduce the flow of methane.

ACKNOWLEDGMENT: The authors wish to thank the Gas Research Institute for supporting this work under contract number 5090-260-2003.

REFERENCES

Barton, N.R. 1972. A model study of air transport from underground openings situated below groundwater level. In Proceedings Symposium International Society for Rock Mechanics. Suttgart. Deutsche Geselischaft für Erd-und Grundbau. T3-A1-T3-A20.

Bawden, W.F. & Rogiers, J.C. 1985. Gas escape from undergtound mined storage facilities - A multiphase flow phenomena. In Proceedings International Symposium on Fundamentals of Rock Joints. Edited by O. Stephansson. Center Publishers. Norway. 503-514.

Evans, D.D. 1983. Unsaturated flow and transport through fractured rock - related to high-level waste repositories. Final Report-Phase I. Dept. Hydrology and Water Resources. University of Arizona. Report NUREG/CR-3206.

Evans, D.D. & Huang, C.H. 1983. Role of desaturation on transport through fractured rock. In Role of Unsaturated Zone in Radioactive and Hazardous Waste Disposal. Eds. J.W. Mercer, P.S.C. Rao & I. Marine. Ann Arbor Science. 165-178.

Fuerstenau, D.W., J. Diao & J.S. Hanson 1990. Estimation of the distribution of surface sites and contact angles on coal particles from film flotation data. Am. Chem. Soc. 4:34-37.

Halperin, B.I., Feng, S. & Sen, P.N. 1985. Differences between lattice and continuum percolation transport exponents. Phys. Rev. Lett. 54:2391.

Merrill, L.S., Jr. 1975. Two-phase flow in fractures. PH.D. thesis. Univ. of Denver. Denver. Colo.

Nolte, D.D. & L.J. Pyrak-Nolte 1991. Stratified continuum percolation: scaling geometry of hierarchical cascades. Phy. Rev. A. 44:6320-6333.

Pruess, K. & Tsang, Y.V. 1990. On two-phase relative permeability and capillary pressure of rough-walled rock fractures. Water Res. Res. 26:1915-1926.

Pyrak-Nolte, L.J., Cook, N.G.W. & Nolte, D.D. 1988. Fluid percolation through single fractures. Geophys. Res. Lett. 15:1247-1250.

Pyrak-Nolte, L.J., D.D. Nolte, L.R. Myer & N.G.W. Cook 1990. Fluid flow through single fractures. In Rock Joints. Edited by Barton & Stephansson. A.A. Balkema. Rotterdam. 405-412.

Rasmussen, T.C., Huang, C.H. & Evans, D.D. 1985. Numerical experiments on artificially generated, three-dimensional fracture networks: an examination of scale and aggregation effects. Mem. Int. Assoc. Hydrogeol.. XVII:676-682.

Rasmussen, T.C. 1987. Computer simulation model of steady fluid flow and solute transport through three-dimensional fracture networks of variably saturated discrete fractures. In Flow and Transport through Unsaturated Fractured Rock. Edited by Evans & Nicholson. Geophysical Monograph 42. American Geophysical Union. 107-114.

Witherspoon, P.A., Wang, J.S.Y., Iwai, K. & Gale, J.E. 1980. Validity of cubic law for fluid flow in a deformable rock fracture. Water Res. Res. 16:1016-1024.

Wong, P-Z. 1988. The statistical physics of sedimentary rocks. Physics Today. 41:24-32.

Tillerson, J.R. & W.R. Wawersik (eds.) 90 5410 045 1
Rock mechanics: Proceedings of the 33rd US Symposium – *Sweeney Convention Center / Santa Fe, NM / 3 – 5 June 1992*
1992, 23 cm, 1200 pp., Hfl.150 / $85.00 / £47
Origin of stresses in the lithosphere; Rock mass monitoring; Blasting; Reservoir completion & stimulation; Fluid & contaminant transport; Fault mechanics; Subsidence & ground motions; In situ storage & sealing; Geothermal energy; Case histories; Numerical methods; Nonlinear dynamic systems; Fracture mechanics; Experimental methods; Constitutive modelling & strain localization; Geostatistics & reliability; Physical rock properties; Geotechnical design methodology; Underground imaging; Induced seismicity; Modelling of fractured reservoirs.

FROM THE SAME PUBLISHER:

Roegiers, Jean-Claude (ed.) 90 6191 194 X
Rock mechanics as a multidisciplinary science – *Proceedings of the 32nd US symposium on Rock Mechanics, Norman, Oklahoma, 10 – 12 July 1991*
1991, 23 cm, 1236 pp., Hfl.150 / $85.00 / £47
In situ stresses; Instrumentation / Measurement techniques; Fracturing; Rock properties; Dynamics / Seismicity; Modelling; Laboratory testing; Analysis; Field observation; Wellbore stability; Design; Discontinuities / Fluid flow; Lunar rock mechanics. Editor: University of Oklahoma, Norman.

Hustrulid, W. & G.A. Johnson (eds.) 90 6191 123 0
Rock mechanics contributions and challenges – *Proceedings of the 31st US symposium on rock mechanics, Golden, Colorado, 18 – 20 June 1990*
1990, 23 cm, 1060 pp., Hfl.185 / $99.00 / £58
The Canadian connection; Coal mine stability; Coal mining; Coal strata; Discontinuities; Fracture mechanics; Hard core modeling; Hydro-geology; In-situ testing; Jointed rock; Mechanical fragmentation; Metal mining; Mine subsidence; New instruments; New laboratory testing techniques; Oil & gas; Open pit mining; PC based modeling of practical problems; QA effects; Reinforcement; Remote sensing/Borehole geophysics; Rock blasting; Rock bursts; Rock deformation; The Scandinavian connection; etc. 127 papers. Editors: Colorado School of Mines, Golden & US Bureau of Mines, Denver.

Khair, A.Wahab (ed.) 90 6191 871 5
Rock mechanics as a guide for efficient utilization of natural resources – *Proceedings of the 30th US Symposium, West Virginia, 19–22.06.1989*
1989, 23 cm, 1000 pp., Hfl.185 / $99.00 / £58
A state of the art in the science & engineering aspects of rock mechanics in various topical areas. Understanding the state of the art at the present time & directing future developments is essential in utilizing rock mechanics as a tool for efficient use of our natural resources. The symposium theme is focussed on 3 topical areas: Mining & excavation; Drilling & exploration; Underground storage. 115 papers. Editor: West Virginia University, Morgantown.

P.A.Cundall, R.L. Sterling & A.M. Starfield (eds.) 90 6191 835 9
Key questions in rock mechanics – *Proceedings of the 29th US symposium on rock mechanics, Minneapolis, 13–15 June 1988*
1988, 23 cm, 850 pp., Hfl.185 / $99.00 / £58
An ISRM-sponsored symposium. Experimental studies (laboratory/field); Conceptual, analytical & numerical modeling; Design/Construction methods.

Farmer, Ian W., J.J.K. Daemen, C.S. Desai, C.E.Glass & S.P.Neuman (eds.) 90 6191 699 2
Rock mechanics: Proceedings of the 28th US symposium, *Tucson, Arizona, 29 June – 1 July 1987*
1987, 23 cm, 1264 pp., Hfl.185 / $99.00 / £58
Remote sensing; Rock characterization; Rock testing; Field testing; Exploration & construction case histories; Rock fracture & thermomechanical behavior; Fluid flow & coupled flow in rock masses; Constitutive models & numerical modeling; Scale model studies; Hydrofracture & wellbore stability; Deformation of underground openings; Rock blasting & fragmentation; Rock excavation; Slope stability; Geologic repository design; Mining coal; Mining hardrock. 134 papers.

Ashworth, Eileen (ed.) 90 6191 300 3
Research & engineering applications in rock masses – *26th US symposium on rock mechanics, 26–28 June 1985, South Dakota School of Mines & Technology, Rapid City*
1985, 23 cm, 1340 pp., 2 vols, Hfl.195 / $108.00 / £60
142 papers from USA, Europe, Australia, Asia & Canada on: Slope stability; Geological & empirical evaluation of rock properties; Numerical modeling of fractured rock; Subsidence; Rock mass characterization in deep boreholes.

Brummer, Richard (ed.) 90 6191 153 2
Static and dynamic considerations in rock engineering – *Proceedings of the ISRM international symposium, Swaziland, 10 – 12 September 1990*
1990, 25 cm, 410 pp., Hfl.175 / $95.00 / £55
Rockbursts prediction & control; Tunnelling in slaking & deteriorating rock types; In situ stress measurement; Blast modelling; Rock boreability & cutability; Techniques & problems in deep exploration hole & well drilling. 41 papers.

Barton, Nick & Ove Stephansson (eds.) 90 6191 109 5
Rock joints – *Proceedings of a regional conference of the International Society for Rock Mechanics, Loen, 4–6.06.1990*
1990, 25 cm, 820 pp., Hfl.195 / $108.00 / £60
Rock joint behaviour impacts many branches of engineering including surface & underground mining, dam foundations, tunneling for hydropower & transport, petroleum reservoirs & nuclear waste storage. The subject is in a very active stage of development, and engineers, geologists and scientists involved in these developments have indicated by their 110 papers that rock joints are of great importance in many fields of engineering. Selected papers span 5 continents & 30 countries. Topics covered: Geologic aspects of joint origin & morphology, mechanical, hydraulic & dynamic behaviour. The influence of water flow on frictional strength & the effect of joint deformation on water flow are also strongly represented.

Pinto da Cunha, A. (ed.) 90 6191 126 5
Scale effects in rock masses – *Proceedings of the first international workshop, Loen, Norway, 7 – 8 June 1990*
1990, 25 cm, 354 pp., Hfl.150 / $85.00 / £47
Scale effects are present whenever the deformability, strength, hydraulic characteristics or internal stress in rock masses have to be determined for research or design purposes. Hence, it is important to know how and how much our test results are affected by the sample dimension. Topics: Scale effects in the determination of the deformability & strength of intact rock and joints; Scale effects in the determination of the deformability and strength of rock masses; Scale effects in the determination of internal stresses in rock masses; etc. 29 papers.

All books available from your bookseller or directly from the publisher:
A.A.Balkema Publishers, P.O.Box 1675, Rotterdam, Netherlands
For USA & Canada: A.A.Balkema Publishers, Old Post Rd, Brookfield, VT, USA